MICROBIOLOGY

Antagonism as a foraging strategy in microbial communities

Astrid K. M. Stubbusch[1,2,3]*†, François J. Peaudecerf[4,5], Kang Soo Lee[6,5], Lucas Paoli[7,8], Julia Schwartzman[9], Roman Stocker[5], Marek Basler[10], Olga T. Schubert[1,2], Martin Ackermann[1,2,11]‡, Cara Magnabosco[3]‡, Glen G. D'Souza[1,2,12,13]‡

In natural habitats, nutrient availability limits bacterial growth. We discovered that bacteria can overcome this limitation by acquiring nutrients by lysing neighboring cells through contact-dependent antagonism. Using single-cell live imaging and isotopic markers, we found that during starvation, the type VI secretion system (T6SS) lysed neighboring cells and thus provided nutrients from lysing cells for growth. Genomic adaptations in antagonists, characterized by a reduced metabolic gene repertoire, and the previously unexplored distribution of the T6SS across bacterial taxa in natural environments suggest that bacterial antagonism may contribute to nutrient transfer within microbial communities in many ecosystems.

Bacteria require nutrients to synthesize cellular building blocks such as nucleotides, amino acids, and fatty acids for growth. In nature, nutrients are often found only at low concentrations or in the form of complex polymers that require specific enzymatic degradation before they can be used. Under such conditions, the biomass of other cells that are rich in common metabolites and cellular building blocks could serve as a valuable nutrient source (*1*). Killing neighboring cells can give access to these nutrients.

Bacteria have evolved various systems to lyse neighboring bacteria by transferring toxins such as the type IV and type VI secretion systems (T4SS and T6SS, respectively) (*2*–*4*). These contact-dependent antagonistic systems are widespread in cultured bacteria (*3*). Their dominant ecological role is usually viewed as mediating competition for space and nutrients (*5*–*7*), leading to their characterization as the "weapons" of bacterial "warfare" (*3, 7*–*11*).

In this study, we investigated whether in addition to their role in killing competitors, contact-dependent antagonism mechanisms enable bacteria to acquire nutrients from target cells. This has been hypothesized previously (*12*, *13*), but a direct role in nutrient foraging has never been shown experimentally for nonpredatory bacteria. We focused on the T6SS, a well-studied bacteriophage-like molecular machinery that enables the transfer of diverse toxins into neighboring cells and is present in ~25% of all sequenced Gram-negative bacteria (*14*). The distribution of T6SS$^+$ taxa across natural environments remains uncharted.

Contact-dependent antagonism enables growth during starvation

To determine whether the biomass of target cells provides a source of nutrients for antagonistic cells, we studied a simple community consisting of the marine isolates *Vibrio cyclitrophicus* ZF270 (target cells) and the T6SS-encoding *Vibrio anguillarum* (formerly known as *Vibrio ordalii*) FS144 (T6SS$^+$ cells) as an ecological model system. We investigated the growth of T6SS$^+$ cells and the lysis of target cells at single-cell resolution within a microfluidic device, where cells can grow in a monolayer in shallow microfluidic chambers (fig. S1). When we provided the T6SS$^+$ cells with a carbon source that they could metabolize, *N*-acetylglucosamine (GlcNAc) (fig. S2), they grew exponentially with a doubling rate of ~0.2 hours^{-1} (Fig. 1, A and B; fig. S3; and movie S1). The doubling rate is a measure that is independent of the initial number of cells per chamber, which varies among chambers (fig. S3). In co-culture with target cells, we observed a similar doubling rate (Fig. 1B and fig. S3). When we provided a carbon source that only the target cells could metabolize (alginate; fig. S2), T6SS$^+$ cells failed to multiply in monoculture but were able to grow in coculture with target cells at a doubling rate of ~0.07 hours^{-1} (Fig. 1B, fig. S3, and movies S2 and *3*).

To investigate whether the growth of T6SS$^+$ cells without a metabolizable carbon source is facilitated by the T6SS-mediated killing of target cells rather than by the exchange of secreted nutrients (cross-feeding), we tested whether the growth was contingent on a functional T6SS. We used a genetic model system, *V. cholerae* 2740-80 and its T6SS-deletion mutant (*15*, *16*), paired with *Escherichia coli* as target cells. Again, we provided T6SS$^+$ cells and target cells in microfluidic chambers with a carbon source that T6SS$^+$ cells could not metabolize (melibiose; fig. S1 and movie S4). We found that the growth rate of the T6SS-deletion mutant population was lower than that of the T6SS$^+$ population (figs. S4 and S5, A and B, and movies S5 and S6), suggesting that T6SS-mediated cell lysis increased the growth of T6SS$^+$ cells under carbon starvation conditions. This finding was confirmed by growth rate measurements in bulk culture experiments (−0.1 and 0.3 hours^{-1} for the T6SS-deletion population and T6SS$^+$ population, respectively; fig. S5C).

To test whether the observed growth increase in T6SS$^+$ cells was caused by the acquisition of nutrients from target cells, we used stable isotope probing–Raman microspectroscopy (*17*). We first labeled *E. coli* target cells with deuterium and then co-cultured them with unlabeled *V. cholerae* T6SS$^+$ cells or the T6SS-deletion mutants. After 9 hours, T6SS$^+$ cells showed significant levels of deuterium incorporation compared with the T6SS-deletion cells (Fig. 1C and fig. S5, D and E), further confirming that the T6SS indeed facilitated access to nutrients.

Slow cell lysis increases the nutrient uptake by surrounding cells

A more detailed examination of T6SS-driven antagonism revealed that lysis was not instantaneous. We observed that the cell shape of attacked target cells changed from rod-shaped to round before bursting, likely because T6SS effectors compromised cell wall integrity (*18*) (tables S2 and S3). These round *V. cyclitrophicus* target cells persisted for 1.43 ± 0.20 hours in alginate medium and for 0.33 ± 0.09 hours in GlcNAc medium before bursting (mean ± 95% confidence interval) (Fig. 2A). By staining cells with propidium iodide (PI), which does not permeate intact cell membranes but can enter cells with leaky membranes (*19*, *20*), we found that round target cells incorporated more PI than target cells in their usual rod shape (Fig. 2B). Together, these findings suggest that the action of carbon-starved T6SS$^+$ cells causes slow lysis of target cells, likely leading to gradual rather than instantaneous nutrient release.

[1]Institute of Biogeochemistry and Pollutant Dynamics, Department of Environmental Systems Science, ETH Zurich, Zurich, Switzerland. [2]Department of Environmental Microbiology, Eawag: Swiss Federal Institute of Aquatic Science and Technology, Dübendorf, Switzerland. [3]Geological Institute, Department of Earth and Planetary Sciences, ETH Zurich, Zurich, Switzerland. [4]Univ Rennes, CNRS, IPR (Institut de Physique de Rennes) - UMR 6251, Rennes, France. [5]Institute of Environmental Engineering, Department of Civil, Environmental and Geomatic Engineering, ETH Zurich, Zurich, Switzerland. [6]Department of Mechanical Engineering, Ulsan National Institute of Science and Technology (UNIST), Ulsan, South Korea. Ulsan, South Korea. [7]Department of Biology, Institute of Microbiology and Swiss Institute of Bioinformatics, ETH Zurich, Zurich, Switzerland. [8]Global Health Institute, School of Life Sciences, École Polytechnique Fédéral de Lausanne (EPFL), Lausanne, Switzerland. [9]Department of Biological Sciences, University of Southern California, Los Angeles, USA. [10]Biozentrum, University of Basel, Basel, Switzerland. [11]Laboratory of Microbial Systems Ecology, School of Architecture, Civil and Environmental Engineering (ENAC), École Polytechnique Fédéral de Lausanne (EPFL), Lausanne, Switzerland. [12]Center for Fundamental and Applied Microbiomics, Biodesign Institute, Arizona State University, Tempe, AZ, USA. [13]School of Molecular Sciences, Arizona State University, Tempe, AZ, USA. ***Corresponding author. Email: astrid.stubbusch@monash.edu** †Present address: Department of Microbiology, Biomedicine Discovery Institute, Monash University, Clayton, VIC, Australia. ‡These authors contributed equally to this work.

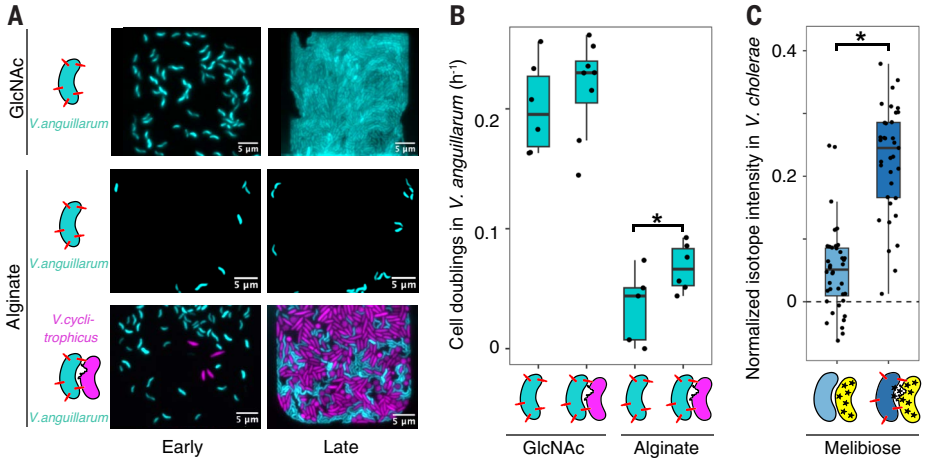

Fig. 1. Growth benefit and acquisition of nutrients released by contact-dependent antagonism through the T6SS. (**A**) Representative images of T6SS$^+$ cells (*V. anguillarum* FS144, cyan) and target cells (*V. cyclitrophicus* ZF270, magenta) supplied with different carbon sources in microfluidic chambers at the start (0 hours) and end time point (12, 24, and 24 hours, top to bottom, respectively, based on the time it took for *V. anguillarum* cells to fill the chamber). Scale bar, 5 µm. (**B**) Growth rate of T6SS$^+$ cells (*V. anguillarum* FS144) in microfluidic chambers estimated from the exponential increase of cell numbers over time shown in fig. S3. Points show the estimates from individual growth chambers (fig. S3), and box plots indicate the median and interquartile range ($n = 6, 8, 5$, and 6 chambers, respectively (left to right); asymptotic Wilcoxon-Mann-Whitney tests, $P = 0.04$). (**C**) Isotope incorporation by *V. cholerae* without T6SS (light blue) and with T6SS (dark blue) from deuterium-labeled *E. coli* (yellow). The deuterium signal in individual *V. cholerae* cells was quantified using Raman microspectroscopy. The co-culture medium contained deuterium and melibiose as a carbon source for the continued growth of labeled *E. coli*. The values were normalized by subtracting the signal of the respective *V. cholerae* cells in this medium in monoculture (fig. S5E). T6SSs are shown as red spikes and deuterium as star symbols ($n = 40$ and 35 cells, respectively (left to right); Wilcoxon rank-sum tests, $P = 8 \times 10^{-13}$).

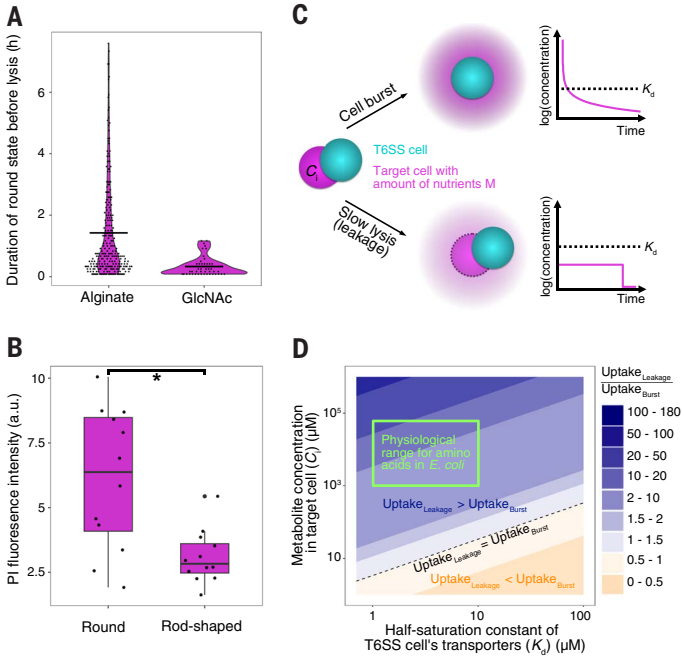

Fig. 2. Slow cell lysis increases the nutrient gain for T6SS cells. (**A**) *V. anguillarum* T6SS cells lyse the *V. cyclitrophicus* target cells slowly, especially under starvation conditions in alginate medium. (**B**) Induction of a round shape in target cells is associated with leakiness of the cell membrane, as estimated by the PI staining intensity of round (length-to-width ratio of 1 to 1.8) and rod-shaped (length-to-width ratio of >1.8 to 6) target cells. Each dot represents the mean value from one microfluidic chamber (from two independent experiments with six chambers each). Jitter was applied in the horizontal direction ($n = 12$ chambers for round and rod-shaped cells; Wilcoxon signed-rank exact test, $P = 5 \times 10^{-4}$). (**C**) Schematic diagram of the mathematical model comparing the nutrient concentration field available to T6SS cells through fast lysis (top) or slow lysis (bottom), alongside the nutrient release from the target cell over time (right). (**D**) Model predictions comparing the approximated total nutrient uptake by an antagonistic cell through slow and fast cell lysis, suggesting that slow lysis increases nutrient uptake in the physiological parameter range. For slow lysis, we assume that the surface concentration of leaked metabolites is small compared with K_d of the T6SS cell. The green box depicts literature values for C_i and K_d in *E. coli* (table S4).

To test whether slow cell lysis improves nutrient acquisition from target cells, we modeled the nutrient concentration field of a cell that bursts instantaneously compared with that of a cell that releases the same amount of nutrients slowly over time (Fig. 2C). We then modeled the nutrient uptake rate of a neighboring T6SS$^+$ cell using Michaelis-Menten kinetics to take into account that membrane transport can reach saturation. Considering the typical intracellular concentration C_i of amino acids and the half-saturation constant K_d of amino acid transporters of *E. coli* (*21*, *22*), we estimated that the approximate total nutrient gain of T6SS$^+$ cells by slow lysis is 2-fold to 50-fold greater than that through fast lysis (Fig. 2, C and D). Fast lysis led to larger initial concentrations of nutrients but exceeded the uptake capacity of the T6SS$^+$ cell's transporters, thus limiting its uptake. T6SS$^+$ cells would acquire more nutrients from a bursting target cell than from a slowly lysing target cell only if the target cell's C_i was >100-fold smaller or the K_d was >10-fold higher than for amino acids in *E. coli*. These results suggest that T6SS$^+$ cells gain more nutrients from slow cell lysis.

We found that the conversion of biomass from slowly lysing cells into new T6SS$^+$ cells was efficient. In densely populated microfluidic chambers, on average, one new T6SS$^+$ cell formed for every two to three lysing target cells (fig. S6B). This biomass conversion was substantially more efficient than that previously reported for various taxa in well-mixed systems, which required 13 to 2000 heat-killed cells for the growth of one new cell (*23*). This high efficiency may partly be explained by the ~2-fold larger volume of the target cells compared with the T6SS$^+$ cells in our system (fig. S6, C to E). However, it also suggests that T6SS$^+$ cells more efficiently acquire nutrients from slowly lysing cells in sessile microbial communities.

Environmental significance of the use of the T6SS for nutrient foraging

If the T6SS is generally used to generate sources of nutrients by lysing cells, then one would expect to observe a reduction of genes needed for the degradation of complex organic matter and synthesis of cellular building blocks, as observed in pathogenic and predatory bacteria (*24*, *25*). To test this idea, we compared the gene repertoire of T6SS$^+$ and T6SS$^-$ genomes within the genus *Vibrio*. We analyzed ~6000 publicly available high-quality genomes. First, we screened the genomes for the presence of a T6SS (fig. S7) and then de-replicated the genomes into 141 operational taxonomic units (OTUs) (fig. S8).

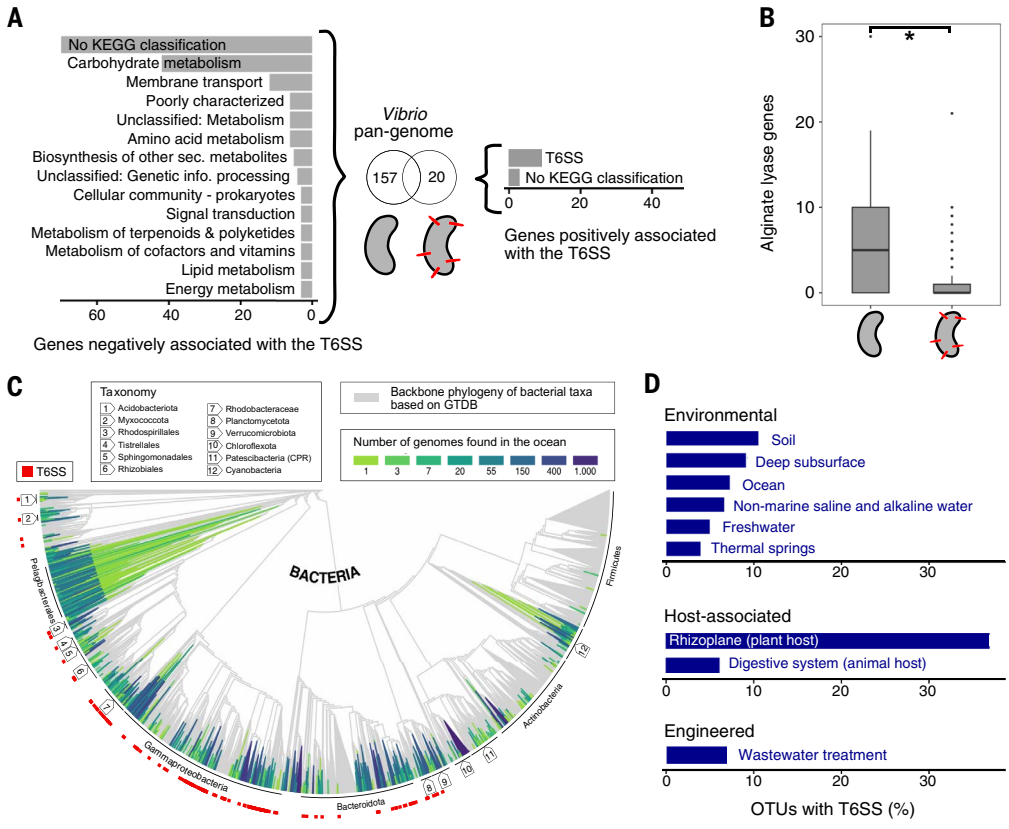

Fig. 3. *Vibrio* with T6SSs have a reduced metabolic gene repertoire, and bacteria with T6SSs are prevalent in natural environments. (**A**) Counts of genes that are positively or negatively associated with the presence of the T6SS in 141 *Vibrio* species-level OTUs, grouped into functional categories according to the Kyoto Encyclopedia of Genes and Genomes (KEGG) classification. A gene can be part of several KEGG classes. Functional categories with fewer than three significant genes are not shown. (**B**) Number of alginate lyase genes across *Vibrio* OTUs with ($n = 82$) and without ($n = 39$) the T6SS (Wilcoxon rank sum test, $P = 1 \times 10^{-5}$). (**C**) Genomes of the OMD (green to blue) placed onto the bacterial Genome Taxonomy Database (GTDB) backbone tree (gray) [modified from Fig. 2C in Paoli *et al.* (*28*)], with red squares indicating the T6SS-encoding genomes. For visualization, the last 15% of the nodes were collapsed (color codes indicate the number of genomes collapsed). (**D**) Prevalence of T6SS-encoding OTUs in different ecosystems based on data from the genomic catalog of Earth's microbiomes (*30*).

We found T6SS$^+$ genomes in 82 OTUs, genomes without T6SS in 39 OTUs, and 20 OTUs that had both T6SS$^+$ and T6SS$^-$ genomes (fig. S9). A pan-genome–wide association study (*26*) on representative genomes of the 82 T6SS$^+$ and 39 T6SS$^-$ OTUs was used to identify T6SS-associated genes. Because many bacterial traits are conserved among related taxa, we removed associations that arose from the underlying phylogenetic structure of the OTUs using a post hoc label-switching permutation test (*26*) (fig. S10). We found 20 genes that had significantly positive and 157 genes that had significantly negative associations with the T6SS. The genes positively associated with the T6SS primarily encode the T6SS itself (Fig. 3A). The genes negatively associated with the T6SS are mainly involved in metabolic processes such as carbohydrate metabolism, metabolite transport, amino acid metabolism, and biosynthesis of secondary metabolites (Fig. 3A). This finding indicates that these metabolic functions are reduced in T6SS$^+$ species. As an example, for carbohydrate metabolism, we found that T6SS$^+$ *Vibrio* genomes contained significantly fewer enzymes to degrade alginate (1.54 ± 0.75 alginate lyases in T6SS$^+$ and 6.03 ± 2.24 in T6SS$^-$ genomes) (Fig. 3B and fig. S11E), and the pan-genomic association study showed that alginate lyases of the PL7, PL12/PL17, and PL15/35 families were significantly negatively associated with the T6SS. The genome size and genome completeness were, however, not significantly different between T6SS$^+$ and T6SS$^-$ OTUs (fig. S11, A to C). Overall, the reduced repertoire of metabolic genes that we observed, particularly for carbohydrate metabolism, in T6SS$^+$ genomes is consistent with genomic adaptation toward acquisition of nutrients and macromolecules from external sources, rather than their biosynthesis from simple metabolites obtained from the decomposition of complex organic matter.

In the ocean, cell lysis induced by viruses is known to be an important contributor to carbon and nutrient cycling, a phenomenon known as the "viral shunt" (*27*). Cell lysis through bacterial antagonism may enhance this flux of carbon from living bacterial cells to lysis products. Therefore, we screened for T6SS genes in the Ocean Microbiomics Database (OMD) (*28*), a consolidated collection of metagenome-assembled genomes from four major global ocean expeditions and two marine time series, as well as in single-cell amplified genomes and marine microbial isolate genomes (fig. S12). In the combined 7610 bacterial species-level OTUs, we found T6SS in 281 OTUs, i.e., in ~3.7%. In 229 of these OTUs, more than half of the OTU members had a T6SS, i.e., in ~3.0% (Fig. 3C). Apart from clades that are known to be rich in T6SS, such as *Gammaproteobacteria* and *Bacteroidota*, we also found that *Planctomycetota* and *Rhodobacteraceae*, which are abundant in the coastal ocean (*29*), frequently encode T6SS. Overall, the prevalence of the T6SS in marine taxa from the global oceans suggests that T6SS-mediated nutrient foraging is common and may thus substantially influence nutrient cycling in the ocean.

A wider screen of natural environments showed that T6SS$^+$ bacteria are common in diverse habitats. We screened for the presence of T6SS genes in a catalog of Earth's microbiomes containing 45,599 species-level OTUs that include metagenome-assembled bacterial genomes from >10,000 samples from diverse habitats (*30*). We found T6SS genes in 4 to 7% of OTUs in aquatic systems, in 9 to 11% of OTUs in terrestrial systems, and in 37% of OTUs in the rhizoplane (Fig. 3D). This is consistent with previous findings suggesting that T6SS$^+$ bacteria are more common among particle-attached than among planktonic bacteria (*13*). In addition, soils have the largest average number of cells per volume of any known ecological environment (*31*, *32*), and the rhizosphere is considered to be the richest niche within this habitat (*5*, *33*), which may promote contact-dependent interactions in this environment. In the rhizoplane, most bacteria are thought to be commensals, but plant pathogens were found that use the T6SS to dominate the root microbiota and increase their virulence against the host plant (*5*). In environments that are comparatively rich in organic biomass, such as the digestive systems of animals and wastewater treatment plants, 6 and 7% of OTUs were T6SS$^+$, respectively. These

findings indicate that the T6SS is widespread across both nutrient-rich and nutrient-poor natural environments.

Discussion

In this work, we found that contact-dependent antagonism can be used by bacteria to access nutrients from cell lysate, which can be rapidly assimilated at low metabolic cost. In contrast to the difficult-to-digest, complex organic compounds prevalent in natural environments, such as polysaccharides, this source contains many readily available cellular building blocks, such as nucleotides and amino acids (25 and 57% of cell content, respectively) (*34*). Directly polymerizing these building blocks into functional cell components represents an energy savings of >90% compared with first having to synthesize them and also reduces proteomic cost (*34*). This mode of nutrient foraging is likely effective in microbial communities with a high frequency of cell-cell contact and limited diffusional loss of released nutrients, such as those in biofilms, soil aggregates, marine snow, the rhizosphere, and the intestinal mucus layer. It is less likely to bring an advantage in planktonic cells, but we have not assessed the efficiency of nutrient foraging in planktonic cells.

Nutrient foraging is an alternative to the mediation of bacterial competition and other functions that have been ascribed to the T6SS, such as acquisition of genetic material (*12*), defense (*35*), and metal scavenging (*36*). These functions are not mutually exclusive, but the genomic signatures of T6SS$^+$ species in *Vibrio* match the expectations that arise from a role in nutrient foraging (*24*, *25*). Nonetheless, it remains unknown whether antagonistic foraging in bacterial communities is the cause of this genomic adaptation or if other factors dominate. For example, some T6SSs are active against eukaryotic hosts (*9*), which may contribute to an association between T6SSs and the reduced metabolic capacity in a host-associated lifestyle. The reduced repertoire of enzymes for carbohydrate degradation renders cells unable to grow on certain carbon sources, such as alginate in the case of *V. anguillarum*. In these conditions, they are not in competition with other cells for the carbon source, but the possession of a T6SS enables them to acquire carbon from nearby cells, thus extending their ecological niche. Functional and genomic analyses of other genera are now necessary to determine whether this function is important in other T6SS-encoding taxa. Under a broad definition of predation, i.e., killing cells for nutrient uptake, this interaction may be classified as facultative predation; however, there is no evidence that T6SS$^+$ cells actively hunt target cells, so this does not meet the stricter definitions of predation (*37*). In contrast to predation through ixotrophy, a recently described hunting strategy found in some filamentous T6SS$^+$ bacterial species of the *Saprospiria* and *Cytophagia* classes with "grappling hooks" to attach to prey cells (*38*), the T6SS$^+$ cells studied here did not grasp target cells.

Because the T6SS is found in diverse taxa and diverse environments, we expect interbacterial cell lysis to also affect large-scale biogeochemical processes. Cell lysis releases both labile dissolved organic matter and carbon-rich particulate organic matter (*27*). The pool of labile substances provided by the lysate can be readily reused by bacteria (*39*), whereas the more recalcitrant particulate organic matter may preferentially sink into deeper ocean layers and thus contribute toward long-term carbon storage in the ocean, as proposed for the "viral shunt" (*27*). Our analyses suggest that there may be a parallel "bacterial shunt" that participates in marine biogeochemical cycling.

REFERENCES AND NOTES

1. J. E. González-Pastor, E. C. Hobbs, R. Losick, *Science* **301**, 510–513 (2003).
2. S. B. Peterson, S. K. Bertolli, J. D. Mougous, *Curr. Biol.* **30**, R1203–R1214 (2020).
3. E. T. Granato, T. A. Meiller-Legrand, K. R. Foster, *Curr. Biol.* **29**, R521–R537 (2019).
4. T. A. Klein, S. Ahmad, J. C. Whitney, *Trends Microbiol.* **28**, 387–400 (2020).
5. R. Gallegos-Monterrosa, S. J. Coulthurst, *FEMS Microbiol. Rev.* **45**, fuab033 (2021).
6. D. L. MacIntyre, S. T. Miyata, M. Kitaoka, S. Pukatzki, *Proc. Natl. Acad. Sci. U.S.A.* **107**, 19520–19524 (2010).
7. M. Basler, B. T. Ho, J. J. Mekalanos, *Cell* **152**, 884–894 (2013).
8. B. W. Anderson, J. D. Wang, *Nature* **575**, 599–600 (2019).
9. S. Coulthurst, *Microbiology* **165**, 503–515 (2019).
10. R. E. Hernandez, R. Gallegos-Monterrosa, S. J. Coulthurst, *Cell. Microbiol.* **22**, e13241 (2020).
11. T. G. Sana, K. A. Lugo, D. M. Monack, *PLOS Pathog.* **13**, e1006325 (2017).
12. S. Borgeaud, L. C. Metzger, T. Scrignari, M. Blokesch, *Science* **347**, 63–67 (2015).
13. M. W. Kempnich, M. P. Sison-Mangus, *PLOS ONE* **15**, e0244217 (2020).
14. F. Boyer, G. Fichant, J. Berthod, Y. Vandenbrouck, I. Attree, *BMC Genomics* **10**, 104 (2009).
15. M. Basler, J. J. Mekalanos, *Science* **337**, 815 (2012).
16. J. P. Schneider *et al.*, *EMBO J.* **38**, e100825 (2019).
17. K. S. Lee *et al.*, *Nat. Rev. Methods Primers* **1**, 80 (2021).
18. T. Dörr, B. M. Davis, M. K. Waldor, *PLOS Pathog.* **11**, e1004850 (2015).
19. L. Boulos, M. Prévost, B. Barbeau, J. Coallier, R. Desjardins, *J. Microbiol. Methods* **37**, 77–86 (1999).
20. C. Kirchhoff, H. Cypionka, *J. Microbiol. Methods* **142**, 79–82 (2017).
21. A. J. Roe, D. McLaggan, I. Davidson, C. O'Byrne, I. R. Booth, *J. Bacteriol.* **180**, 767–772 (1998).
22. J. R. Piperno, D. L. Oxender, *J. Biol. Chem.* **243**, 5914–5920 (1968).
23. I. Nioh, A. Furusaka, *J. Gen. Appl. Microbiol.* **14**, 373–385 (1968).
24. V. Merhej, M. Royer-Carenzi, P. Pontarotti, D. Raoult, *Biol. Direct* **4**, 13 (2009).
25. Z. Pasternak *et al.*, *ISME J.* **7**, 756–769 (2013).
26. O. Brynildsrud, J. Bohlin, L. Scheffer, V. Eldholm, *Genome Biol.* **17**, 238 (2016).
27. C. A. Suttle, *Nat. Rev. Microbiol.* **5**, 801–812 (2007).
28. L. Paoli *et al.*, *Nature* **607**, 111–118 (2022).
29. B. J. Campbell, L. Yu, J. F. Heidelberg, D. L. Kirchman, *Proc. Natl. Acad. Sci. U.S.A.* **108**, 12776–12781 (2011).
30. S. Nayfach *et al.*, *Nat. Biotechnol.* **39**, 499–509 (2021).
31. P. D. Schloss, J. Handelsman, *PLOS Comput. Biol.* **2**, e92 (2006).
32. L. F. W. Roesch *et al.*, *ISME J.* **1**, 283–290 (2007).
33. A. M. Hirsch, *Symbiosis* **37**, 345–363 (2004).
34. M. A. Lever *et al.*, *FEMS Microbiol. Rev.* **39**, 688–728 (2015).
35. S. Pukatzki *et al.*, *Proc. Natl. Acad. Sci. U.S.A.* **103**, 1528–1533 (2006).
36. X. Yang, H. Liu, Y. Zhang, X. Shen, *Front. Microbiol.* **12**, 756136 (2021).
37. J. Pérez, A. Moraleda-Muñoz, F. J. Marcos-Torres, J. Muñoz-Dorado, *Environ. Microbiol.* **18**, 766–779 (2016).
38. Y.-W. Lien *et al.*, *Science* **386**, eadp0614 (2024).
39. I. Beidler *et al.*, *Nat. Commun.* **15**, 4048 (2024).
40. A. K. M. Stubbusch, Code and data for: Antagonism as a foraging strategy in microbial communities, ERIC Open (2025); https://doi.org/10.25678/000D09.
41. A. K. M. Stubbusch, Stable isotope probing Raman microspectroscopy data for: Antagonism as a foraging strategy in microbial communities, MicrobioRaman (2025); https://www.ebi.ac.uk/biostudies/microbioraman/studies/S-MBRS13.

ACKNOWLEDGMENTS

We thank current and previous members of the Schubert and Ackermann and Magnabosco labs, the PriME collaboration, and M. Gabrielli for helpful discussions; H. Wildschutte for providing the antibiotic deletion of *V. anguillarum*; F. Oschmann and J. Fluri for the development of the segmentation and tracking tool *MIDAP*; K. Drescher and N. Netter for advice on single-cell segmentation of the T6SS cells; and R. Naisbit for editorial comments. We declare the use of ChatGPT-4 to inspire specific coding solutions. **Funding:** This work was supported by ETH Zurich and Eawag (M.A., O.T.S.); Simons Foundation grants 542379FY22 and 542395FY22 as part of the Principles of Microbial Ecosystems (PriME) Collaboration (R.S., O.T.S., M.A.) and PriME Opportunity Grant from the PriME Collaboration (G.G.D., J.S.); ETH Zurich (C.M.); ETH fellowship and a Marie Curie Actions for People COFUND program fellowship FEL-3716-1 (G.G.D.); ETH Career SEED grant SEED-14 18-1 (G.G.D.); and Gordon and Betty Moore Foundation Symbiosis in Aquatic Systems Initiative Investigator Award GBMF9197 to R.S.). **Author contributions:** Conceptualization: A.K.M.S., M.A., C.M., G.G.D.; Funding acquisition: M.A., O.T.S., G.G.D., R.S., J.S.; Investigation: A.K.M.S., G.G.D., F.J.P., K.S.L.; Methodology: A.K.M.S., G.G.D., F.J.P., K.S.L., J.S., M.B., L.P.; Project administration: A.K.M.S.; Supervision: M.A., O.T.S., C.M., G.G.D.; Visualization: A.K.M.S.; Writing – original draft: A.K.M.S.; Writing – review & editing: All authors. **Competing interests:** R.S. is also affiliated with PhAST Inc., Zurich. K.S.L. is also affiliated with the Department of Biological Sciences and the Department of Biomedical Engineering, Ulsan National Institute of Science and Technology (UNIST), Ulsan, South Korea. The remaining authors declare no competing interests. **Data and materials availability:** Code and data to reproduce the results and figures in this paper are available on ERIC Open (*40*). The stable isotope probing Raman microspectroscopy data are also deposited in the MicrobioRaman database (*41*).

SUPPLEMENTARY MATERIALS

science.org/doi/10.1126/science.adr8286
Materials and Methods; Figs. S1 to S12; Tables S1 to S8; References (*42*–*76*); Movies S1 to S6; MDAR Reproducibility Checklist

Submitted 19 November 2024; accepted 17 April 2025

10.1126/science.adr8286